Recognition Method Based on Gabor Wavelet Transform and Discrete Cosine Transform

Bo-wen Zheng, Jie-sheng Wang, Yan-lang Ruan, Shu-zhi Gao

Abstract—**A fingerprint recognition method based on Gabor wavelet transform and discrete cosine transform (DCT) was proposed. The multichannel Gabor filters and improved binarization algorithm are adopted to enhance the fingerprint images. The hybrid strategy of the discrete cosine transform method and the Gabor wavelet transform algorithm was proposed to form an improved Gabor wavelet transform applied to the fingerprint feature extraction and feature reduction. Finally, the nearest neighbor distance detector and Euclidean distance are used as classifier to classify the fingerprint. The results of simulation experiments prove that the proposed strategy can effectively shorten the recognition time and maintain a considerable recognition rate.**

Index Terms—**fingerprint recognition, gabor wavelet transform, discrete cosine transform;**

I. Introduction

IN 1892, Sir Francis Galton of England carried out a systematic study on fingerprints and firstly proposed the uniqueness of fingerprint characteristics. Because its uniqueness, fingerprints can be used as identification code. This code cost is almost zero, and the safety factor is high for life. Therefore, the fingerprint recognition is also an important direction of biometric identification [1]. The fingerprint recognition [2-5] mainly includes four stages: fingerprint enhancement [6] (it also known as the fingerprint image prepossessing [7]), fingerprint feature extraction [8-9], fingerprint image classification and compression [10] (in the case of large data), and fingerprint image matching [11-12].

For the grayscale fingerprint image, the ridge line and valley line can be considered as sine wave shape in local small neighborhood with certain frequency and direction [13]. This feature makes the Gabor filter suitable to enhance the fingerprint images [14-15]. Vutipong et al. used a series of independent Gabor filters to enhance the fingerprint image, which is about 2.6 times faster than the traditional Gabor filter. Sherlock et al. proposed a directional filtering algorithm based on frequency domain. Other fingerprint enhancement methods include frequency domain enhancement algorithm based on Fourier transform [16-17], knowledge based fingerprint image enhancement algorithm, which uses the image structure information to guide the image enhancement process [18], the nonlinear diffusion model and its filtering method in texture analysis mode [19-20] and edge extraction [21], the multi-scale filtering, which is introduced of multi-scale space theory in fingerprint enhancement [22]. Fingerprint characteristics includes the overall characteristics and local characteristics. The overall features include: singular point features, type characteristics and spectrum characteristics. Local features include detail point features, sweat pores, texture features and so on. The fingerprint classification techniques mainly include rules, syntax, structure, statistics, neural network, and multiple classifiers, etc. Fingerprint matching algorithms mainly include the fingerprint matching algorithm based on string matching algorithm, the matching algorithm based on the details of the distance, the matching algorithm based on triangle structure, matching algorithm based on topology, the matching algorithm based on point pattern [23-24], etc.

In this paper, the fingerprint images are enhanced by Gabor filter. This Gabor filter can adaptively adjust various parameters according to different blocks of fingerprints. In fact, the multi-channel Gabor filters with different parameters are used to enhance the fingerprint image, then the enhanced image is refined. The Gabor wavelet filter is used to extract the fingerprint feature again, and the feature dimension reduction is carried out by the DCT method. Finally, the nearest neighbor classifier and the Euclidean distance are used to classify and identify the pictures.

II. Fingerprint Enhancement

A. Fingerprint Normalization Processing

As the fingerprint collection device itself or the pressure of the finger is uneven, the fingerprint image will change too much in the direction of the ridge or valley. Therefore it is necessary to normalize the fingerprint image. The purpose of fingerprint image normalization is to reduce the degree of gray change along the ridge line and valley direction, without changing the clear contrast of the ridge line and the grain structure. The fingerprint image is I. m and n are width and height, respectively. $I(i,j)$ means the the grayscale value at i th line and j th column. $M(I)$ is the average of grays and

Manuscript received January 11, 2018; revised April 12, 2018. This work was supported by the the Basic Scientific Research Project of Institution of Higher Learning of Liaoning Province (Grant No. 2017FWDF10), the Program for Research Special Foundation of University of Science and Technology of Liaoning (Grant No. 2015TD04) and the Opening Project of National Financial Security and System Equipment Engineering Research Center (Grant No. USTLKFGJ201502).

Bo-Wen Zheng is with the School of Electronic and Information Engineering, University of Science and Technology Liaoning, Anshan, 114051, PR China (e-mail:18842038281@163.com).

Jie-Sheng Wang is with the School of Electronic and Information Engineering, University of Science and Technology Liaoning, Anshan, 114051, PR China; National Financial Security and System Equipment Engineering Research Center, University of Science and Technology Liaoning. (phone: 86-0412-2538246; fax: 86-0412-2538244; e-mail: wang_jiesheng@126.com).

Yan-lang Ruan is with the School of Electronic and Information Engineering, University of Science and Technology Liaoning, Anshan, 114051, PR China (e-mail:ruanyanlang@163.com).

Shu-Zhi Gao is with Shenyang University of Chemical Technology, Shenyang, 110000, PR China (e-mail: szg6868@126.com).

$VAR(I)$ represents the standard deviation, which can be expressed as:

$$M(I) = \frac{1}{m * n}\sum_{i=0}^{m-1}\sum_{j=0}^{n-1} I(i,j) \tag{1}$$

$$VAR(I) = \frac{1}{m*n}\sum_{i=0}^{m-1}\sum_{j=0}^{n-1}\left(I(i,j) - M(I)\right)^2 \tag{2}$$

After normalization, the fingerprint image can be expressed as follows:

$$G(i,j) = \begin{cases} M_0 + \sqrt{\dfrac{VAR_0\left(I(i,j) - M(I)\right)^2}{VAR}}, I(i,j) > M \\ M_0 - \sqrt{\dfrac{VAR_0\left(I(i,j) - M(I)\right)^2}{VAR}}, Other \end{cases} \tag{3}$$

The above method in this paper is simplified as:

$$G = \frac{I - M}{VAR} \tag{4}$$

The images in the CASIA fingerprint library is adopted to carry out this experiment. The result of the fingerprint normalization experiment is shown in Fig. 1 and Fig. 2.

B. Fingerprint Direction Field

The orientation diagram is actually a transformation of the original fingerprint image, which means the direction of the grain line in a certain direction of the line. The Gabor filters are used to enhance the fingerprint images according to the direction diagram, so the direction of the calculation is crucial.

Fig. 1 Traditional methods normalization.

Fig. 2 Simplified normalization.

In this paper, the direction graph is solved by the method of shaving operator. The detailed algorithm is described as follows.

Step 1: The fingerprint image G is divided into blocks, whose size is $W \times W$.

Step 2: The gradient $\partial_x(i,j)$ and $\partial_y(i,j)$ of its pixels for each block are calculated based on the following equations.

$$\partial_x(i,j) = \sum_{u=-1}^{1}\sum_{v=-1}^{1} S_x(u+1, v+1) G(i-u, i+v) \tag{5}$$

$$\partial_y(i,j) = \sum_{u=-1}^{1}\sum_{v=-1}^{1} S_y(u+1, v+1) G(i+u, i+v) \tag{6}$$

where, S_x and S_y represent the Soble operator.

Step 3: According to the Eq. (5) and (6), the gradient value gives the block direction.

$$V_x(i,j) = \sum_{u=i-w/2}^{i+w/2}\sum_{v=j-w/2}^{j+w/2} 2\partial_x(u,v)\partial_y(u,v) \tag{7}$$

$$V_y(i,j) = \sum_{u=i-w/2}^{i+w/2}\sum_{v=j-w/2}^{j+w/2}\left(\partial_x^2(u,v) - \partial_y^2(u,v)\right) \tag{8}$$

$$\text{If } V_x(i,j) \neq 0, \quad \theta(i,j) = \frac{1}{2} \times \arctan\left(V_y(i,j)/V_x(i,j)\right) \tag{9}$$

$$\text{If } V_x(i,j) = 0, \quad \theta(i,j) = \pi/2 \tag{10}$$

Repeat Step 3 and 3 until all the directions of the blocks are calculated.

Step 4: Smooth the direction graph. Because the trend of the fingerprint lines tends to continuous changes, the adjacent direction should not have a sudden turning point. So it needs to smooth the direction graph.

Set W as 10, 15, 20, and 30, respectively. The calculated direction graphs for different W are shown in Fig. 3.

(a) W=10

(b) W=10

(c) W=10

(d) W=10

Fig. 3 Direction field of fingerprint.

III. Improved Binarization Algorithm Based on Orientation and Frequency

A. Fingerprint Normalization Processing

The most gradual change in the grey degree of the fingerprint image is the direction of the grain line, while the gradient direction is the opposite, which is the fastest changing direction of gray value. With the direction of the grain line as the normal direction and the gray value of each pixel in the direction of the normal line, the waveform of the approximate sine wave can be obtained. Because of this feature of fingerprint images, the Gabor filter can be used to process the fingerprint image, and this filter needs to determine three parameters: the central frequency of the filter, the direction of the filter, and the standard deviation of the Gaussian function σ_x and σ_y. For the traditional Gabor filter, its parameters are set according to experiences, but for the fingerprint images with different properties, they will not be able to get very good filtering effect, so it is necessary to make improvements on them.

The size of sub-blocks of fingerprint images is 20×20, and the direction of this fingerprint image block is selected as the direction of the window, whose center is point (i,j) and size is $l \times w$ (in this paper, w = 20 and l =5). The specific calculation equations are shown as follows.

$$Z[k] = \frac{1}{w}\sum_{d=0}^{w-1} I(u,v), k = 0,1,\ldots l-1 \tag{11}$$

$$u = i + \left(d - \frac{w}{2}\right)\cos\theta(i,j) + \left(k - \frac{l}{2}\right)\sin(i,j) \tag{12}$$

$$v = j + \left(d - \frac{w}{2}\right)\sin\theta(i,j) + \left(\frac{l}{2} - k\right)\cos\theta(i,j) \tag{13}$$

If there is no singularity in the direction window, $Z = [k]$ will form a discrete sinusoidal wave, and the sinusoidal frequency is the same as that of the local fingerprint ridge, so the ridged frequency can be obtained from it. At this point the number of pixels between two peaks in the waveform figure, whose frequency is the reciprocal of the sum of the numbers of pixels. $T = (i,j)$ is the the average number of pixels between two consecutive peak, so the frequency is $\Omega(i,j) = 1/T(i,j)$. If there is no continuous spike, the frequency is set as -1 for be distinguished with other effective frequencies.

The operation is carried out on each small piece in the fingerprint image. If the value of the block is not -1, the original value of the block is kept unchanged. If the value of the block is -1, it is necessary to calculate the block with interpolation method, which can be expressed as follows:

$$D'(i,j) = \begin{cases} D(i,j), if D(i,j) \neq -1 \\ \dfrac{\sum_{u=i-1}^{i+1}\sum_{v=j-1}^{j+1} D(u,v)\sigma(D(u,v))}{\sum_{u=i-1}^{i+1}\sum_{v=j-1}^{j+1}\sigma(D(u,v))}, otherwise \end{cases} \tag{14}$$

$$\sigma(x) = \begin{cases} 0, if x < 0 \\ 1, otherwise \end{cases} \tag{15}$$

In the neighborhood, the distance between the lines varies slowly, that to say the local line frequency changes slowly, so the low-pass filtering can be carried out. At this point, the Gabor filter is chosen for filtering. Since it is an improved filter, a constant coefficient is adopted for the standard deviation σ_x and σ_y shown in Eq. (16) and Eq. (17).

$$\sigma_x = k_x \Omega(i,j) \tag{16}$$

$$\sigma_y = k_y \Omega(i,j) \tag{17}$$

where, Ω is the frequency of the ridges.

In this way, a standard deviation is obtained to expressing the image changes locally, which is good for filtering. The standard deviation needs to be carefully configured. It cannot be too large or too small. Too large standard deviation will general create the pseudo-feature points and too small standard deviation will make filter not easy. In this paper, the values of k_x and k_y are 0.5.

In the traditional Gabor filter algorithm, the width and height of the filter are also set to fixed values. Therefore, it is necessary to improve it so that it can change with the local image of the fingerprint. Establish a relationship as follows:

$$w_x = 6\sigma_x \tag{18}$$

$$w_y = 6\sigma_y \tag{19}$$

where, ω_x is the width of the filter and ω_y is the height of the filter. In this way, the size of the filter is associated with the local frequency. For each region, the designed Gabor filter is different.

Through the above series of derivation and settings, the standard deviation and size of filter have been set, and the frequency of the ridge line has also been derived. So the

fingerprint images are filtered by:

$$\varepsilon(i,j)=\sum_{u=-w_x/2}^{w_x/2}\sum_{v=-w_y/2}^{w_y/2}h(u,v,O(i,j),\Omega(i,j))G(i-u,j-v) \tag{20}$$

where, $O=(i,j)$ is the filtered image, $\varepsilon=(i,j)$ is the frequency in corresponding to pixel points, $\Omega=(i,j)$ is the ridge frequency of point (i,j) in $\omega_x\times\omega_y$ range, and $G(i,j)$ is the fingerprint image after normalization.

In addition, the Gabor filter is a single channel. The filtered result is shown in Fig. 4 to Fig. 7. It can be seen from Fig. 5 that the ridge frequency diagram reflects the ridge spacing of the fingerprint. Seen from Fig. 6, the direction of the detected ridge line is correct. Fig. 7 shows the outline of the outer edge of the fingerprint. The texture of the fingerprint image obtained after filtering is also very clear, which indicates that the filtering effect is considerable.

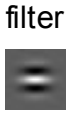

Fig. 4 Gabor filter.

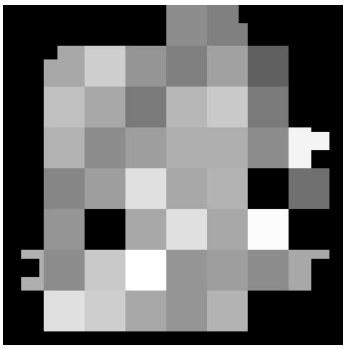

Fig. 5 Ridge frequency.

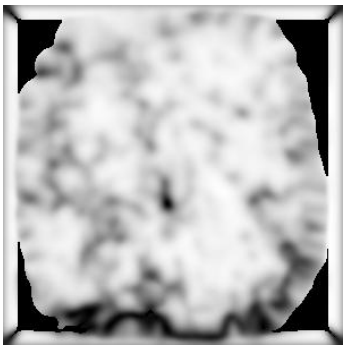

Fig. 6 Degree of reiability.

Fig. 7 Filtered image.

After obtaining the filtered fingerprint images, the binary processing is carried out on therm. The binarization of the images refers to the change of gray image to two values by setting the threshold (0 and 255). The binary image represents the target and background of the image. For the fingerprint images, the binarization is to make the image background and the valley line 255, and the gray value of the image ridge line is 0. Suppose the ridge line direction in point (i,j) is $\theta(i,j)$. The average value of the pixels in one small block whose direction is with $\theta(i,j)$ as the center is w, and the line of the ridged line has a vertical direction of $\theta'(i,j)$. The average value of pixels in a small block centered at this point $\theta'(i,j)$ is w'. While the urine of w and w' can be binary to the fingerprint image, which can be expressed as below:

$$I'(i,j)=\begin{cases}255, if W<W'\\ 0, if W>W'\end{cases} \tag{21}$$

Seen from the above figures, when $W<W'$, it can be determined that this point is above the valley line or background, and its pixel is 255, which is set as white; When $W>W'$, it can be determined that this point is above the ridged line and its pixels are set to 0, which is also called black. The result of binary experiment is shown in Fig. 8.

It can be seen from Fig. 8 that the fingerprint image is binarized with the improved Gabor filter. The outline of the fingerprint is clear, the original image is preserved, and the distortion is not distorted. After binarization, a further refinement is carried out and the processing result shown in Fig.9.

Fig. 8 Binaryzation.

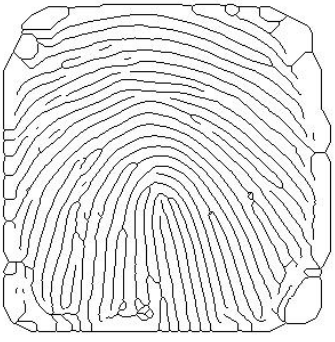

Fig. 9 Fingerprint thinning.

IV. Fingerprint Recognition Method Based on Improved Gabor Wavelet

A. Gabor Wavelet Transform

The essence of Gabor wavelet transform is actually the wavelet transform based on Gabor function, which can be used to analyze the images in various ways. The main principle of Gabor wavelet transform is described as follows. The Gabor function itself constitutes an unorthogonal basis, and a relatively localized frequency description can be obtained with a given base function and its expansion. For this reason, the Gabor function wavelet transform method can be used to extract the fingerprint image features. That is to say that a set of filters with different scales are used to obtain the local characteristics of different scale images.

The two-dimensional Gabor function expression is shown as follows:

$$g(x,y)=\left[\frac{1}{2\pi\sigma_x\sigma_y}\right]\exp\left[-\frac{1}{2}\left(\frac{x^2}{\sigma_x^2}+\frac{y^2}{\sigma_y^2}\right)+2\pi jWx\right] \tag{22}$$

Suppose $g(x,y)$ as a basis function, and expand (x,y). This process is to do a certain degree of rotation and scaling expansion transform so as to obtain the Gabor wavelet, whose specific expression is shown as:

$$g_{m,n}(x,y)=a^{-m}G\left(x^{'},y^{'}\right),a\rangle 1,m,n\in Z \tag{23}$$

where, $\left(x^{'},y^{'}\right)=a^{-m}\left(x\cos\theta+y\sin\theta,-x\sin\theta+y\cos\theta\right)$, M represents the number of directions, and a^{-m} is the scale factor.

By changing M and n, a set of Gabor wavelet filters with different directions and scales can be obtained. However, the obtained wavelet clusters are non-orthogonal to each other. When using it to filter the images, there will be a lot of redundant information. Therefore, when using Gabor wavelet filter to extract fingerprint features, the most crucial step is how to design these parameters of the function. If the parameter is designed reasonably, the redundant information of the image can be made the smallest or the best.

U_L is the minimum frequency of filter center, U_H is the maximum frequency of filter center frequency, M is the number of Gabor wavelet filter directions and S is the Gabor wavelet filter scale. By using the formula $U_H=\alpha^{s-1}U_L$, the scale parameter can be calculated by:

$$\alpha=\left(\frac{U_H}{U_L}\right)^{\frac{1}{s-1}} \tag{24}$$

Eq. (25) can be derived from Eq. (22).

$$U_H-U_L=t+2\alpha t+2\alpha^2t+\ldots+2\alpha^{s-2}t+\alpha^{s-1}t=\frac{\alpha+1}{\alpha-1}\left(\alpha^{2s-1}-1\right)t \tag{25}$$

Because the half amplitude of the Gaussian function of the standard variance δ is $\sigma\sqrt{2ln2}$, the corresponding maximum filter half amplitude is $\alpha^{s-1}t=\sigma_n\sqrt{2ln2}$. This equation is fed into Eq. (24) and (25) to obtain:

$$\sigma_u=\frac{(\alpha-1)U_H}{(\alpha+1)\sqrt{2\ln 2}} \tag{26}$$

According to the existing knowledge, the tangent angle of two adjacent ellipses is $\varphi=\pi/M$, so there is:

$$\frac{(u-U_H)^2}{2\ln 2\sigma_u^2}+\frac{v^2}{2\ln 2\sigma_v^2}=1 \tag{27}$$

Because of $v=tan\frac{\theta}{2}u$, there is also:

$$\left(\sigma_v^2+\tan^2\frac{\phi}{2}\sigma_u^2\right)u^2-2U_H\sigma_v^2u+U_H^2\sigma_v^2-2\ln 2\sigma_u^2\sigma_v^2=0 \tag{28}$$

In the equation of u, the condition that it can have real solutions is described as follows.

$$\sigma_v=\tan\frac{\phi}{2}\sqrt{\frac{U_H^2}{2\ln 2}-\sigma_u^2} \tag{29}$$

Eq. (30) can be obtained from Eq. (28) and Eq. (29).

$$\sigma_v=\tan\left(\frac{\pi}{2M}\right)\left[U_H-2\ln 2\left(\frac{\sigma_u^2}{U_H}\right)-2\ln 2\left(\frac{\sigma_v^2}{U_H}\right)\right]\left[2\ln 2-\frac{(2\ln 2)^2\sigma_H^2}{U_H^2}\right]^{-\frac{1}{2}} \tag{30}$$

After the above derivation, the relationship between the various parameters of the Gabor wavelet filter is very obvious. As long as determine these five parameters (ω, S, M, U_H and U_L), other parameters are able to be calculated out easily. Because the extracted fingerprints are carried out the polar transformation, it makes the Gabor filter have the symmetry. So in the direction of the $[0,\pi]$, the filter can be completely described in the $[0,2\pi]$ direction of the fingerprint information. In this paper, five different frequencies of Gabor wavelet filter (1, $1/\sqrt{2}$, $1/2$, $1/2\sqrt{2}$ and $1/4$) and eight different directions ($\pi/4$, $3\pi/8$, $\pi/2$, $5\pi/8$, $3\pi/4$, $7\pi/8$, 0 and $\pi/8$) are taken. The extracted features are shown in Fig. 10 and Fig. 11.

B. Two-dimensional Discrete Cosine Transform (2D DCT)

The two-dimensional discrete cosine transform is defined as follows:

$$\mathrm{F}(0,0)=\frac{1}{N}\sum_{x=0}^{N-1}\sum_{y=0}^{N-1}f(x,y) \tag{31}$$

$$\mathrm{F}(0,v)=\frac{\sqrt{2}}{N}\sum_{x=0}^{N-1}\sum_{y=0}^{N-1}f(x,y)\cdot\cos\frac{(2x+1)v\pi}{2N} \tag{32}$$

$$F(u,0)=\frac{\sqrt{2}}{N}\sum_{x=0}^{N-1}\sum_{y=0}^{N-1}f(x,y)\cdot\cos\frac{(2y+1)u\pi}{2N} \quad (33)$$

$$F(u,v)=\frac{\sqrt{2}}{N}\sum_{x=0}^{N-1}\sum_{y=0}^{N-1}f(x,y)\cdot\cos\frac{(2y+1)u\pi}{2N}\cdot\cos\frac{(2x+1)v\pi}{2N} \quad (34)$$

where, $f(x,y)$ represents the image space matrix, (x,y) is the current image pixel location, and $F(u,v)$ is the transformation coefficient matrix $(u,v=1,2,...,N-1)$. The two-dimensional discrete transformation is actually to carry out one-dimensional discrete transformations twice. The effect of DCT transformation is shown in Fig. 12.

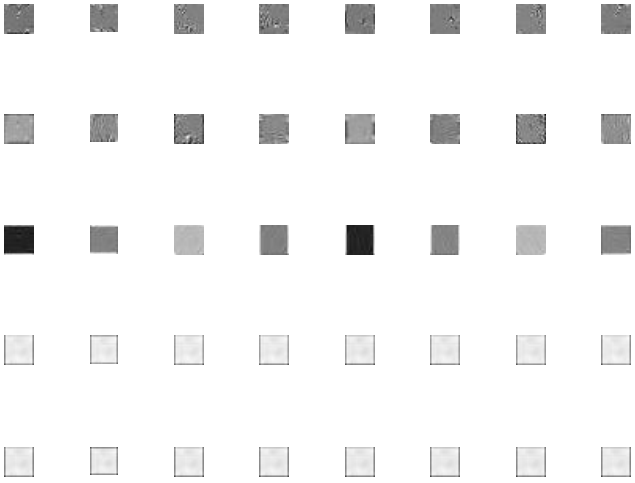

Fig. 10 Real part features.

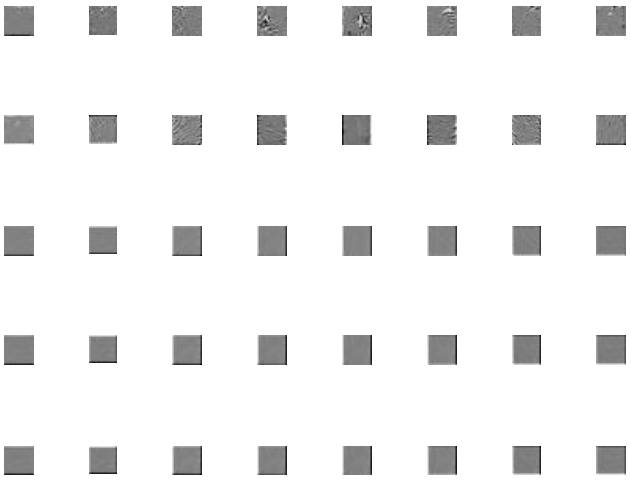

Fig. 11 Imaginary part features.

(a) Original image

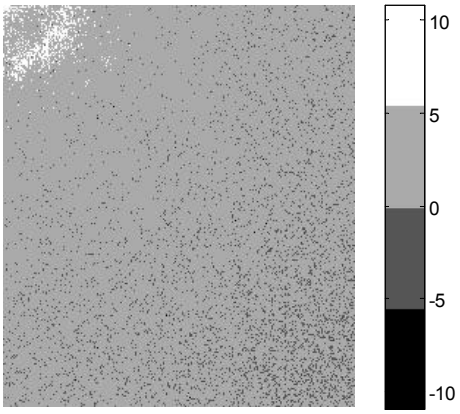

(b) Transformed image

Fig. 12 DCT transform effect.

It can be seen from Fig. 12 that the energy of the transformed DCT coefficients is mainly concentrated in the upper left corner, and the rest of the coefficients are close to zero. This shows that DCT is suitable for the image compression. After the transformation, the DCT coefficient will be limited to the threshold operation, which will be set as zero less than the a certain coefficient. This is the quantization process in image compression, and then the inverse DCT operation will be performed to get the compressed image. In the same way, if the image of Gabor filter is processed with 2D DCT, the effect is shown in Fig. 13.

After carrying out the 2D DCT processing, most of the image energy is focused on the DC part, that is to say it is located in the upper left part of Fig. 13, which can get rid of the correlation between the images well, make the image coding easier and facilitate the feature extraction on the images. Thus, a small amount of information in the upper left corner need be extracted as an effective information for the images, which will greatly compress the images. This is the dimension reduction principle of DCT.

C. Fingerprint Recognition Based on Improved Gabor Wavelet

Seen from the principle of the Gabor wavelet, the Gabor filter can deal with each pixel of the whole image, which will make the Gabor filter recognition rate higher.

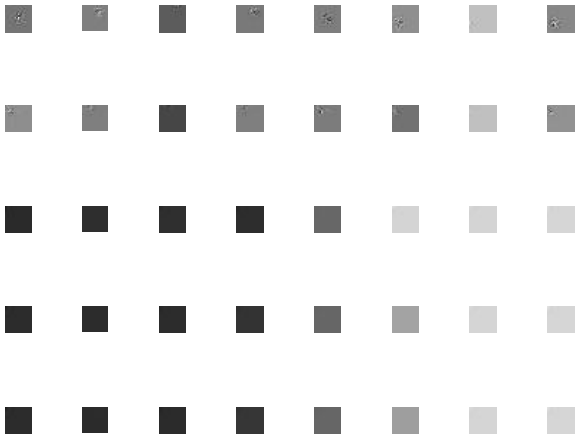

Fig. 13 DCT processing after filtering.

But because not every pixel is a feature point of the image and the feature points occupy only a small part of the image pixels, the Gabor filter has done a great deal of useless work so that the recognition time greatly increases. When using the Gabor filter, how to reduce the recognition time must be considered.

After 2D DCT image processing, the image is mainly concentrated in the DC part. If using 2D DCT for carrying out the image processing firstly, a few parts in the top left corner of the capture image can remove a lot of useless information, and leave behind the main information, which thereby greatly reduces the workload of Gabor filter and the recognition time. So 2D DCT can partially remove the correlation between images, and it is helpful to improve the recognition rate.

In this paper, the idea of improving the Gabor wavelet filter is to process the image through 2D DCT firstly, and capture a few parts of the upper left corner to effectively compress the image. Then the Gabor wavelet is adopted to realize the feature extraction. Thus, the recognition time and the recognition rate are greatly improved to some extent.

V. Fingerprint Identification Classification

A. Minimum Distance Classifier

The minimum distance classifier is one of the most commonly used distance classifier. The class centers of known samples (that is class average) are calculated firstly. Then the unknown samples are classified to the class center with the nearest distance in the class.

In an n-dimensional space, we define A is the name of a category, X_A is the feature set of sample A, x_{An} is the feature set of the n th dimension of category A, μ_A is the mean of A, and μ_{An} is the mean of the n th dimensional feature set. The minimum distance taxonomy firstly calculates the mean $\mu_A = (\mu_{A1},\mu_{A2},\mu_{A3},...,\mu_{An})$ of each known category $X_A = (x_{A1},x_{A2},x_{A3},...,x_{An})$ in each dimension. Similarly, the mean $\mu_B = (\mu_{B1},\mu_{B2},\mu_{B3},...,\mu_{Bn})$ of another category $X_B = (x_{B1},x_{B2},x_{B3},...,x_{Bn})$ is calculated, and then the distance $d(x,\mu_A)$ and $d(x,\mu_B)$ of x to X_A and X_B are computed separately.

B. Distance of Classifier

After the characteristic extraction process, the fingerprint samples finally form the characteristic space composed of these eigenvectors. Therefore, how to calculate the similarity between samples can be realized by calculating distance or Angle. Given vector and , the common similarity measures include:

1) Euclidean distance

$$d(x,y) = \|x-y\| = \sqrt{\sum_{i=1}^{n}(x_i - y_i)^2} \tag{35}$$

2) Block distance

$$d(x,y)\sum_{i=1}^{n}|x_i - y_i| \tag{36}$$

3) Marchwood distance

$$d(x,y) = (x-y)^T C^{-1}(x-y) \tag{37}$$

where, C is the covariance matrix of the pattern, and it can be simplified as:

$$d(x,y) = \sum_{i=1}^{n}\frac{x_i y_i}{\sqrt{\lambda_i}} \tag{38}$$

where λ_I is the variance of the ith component.

4) Angle cosine

$$d(x,y) = \frac{x\cdot y}{\|x\|\|y\|} = \frac{\sum_{i=1}^{n} x_i y_i}{\sqrt{\sum_{i=1}^{n} x_i^2}\sqrt{\sum_{i=1}^{n} y_i^2}} \tag{39}$$

In this article, the Euclidean distance is selected as the classifier.

VI. Simulation Experiments and Results Analysis

Experimental environment: Windows 10-64 bit operating system, Intel(R) Core i5 7th Gen processor, system memory 8G, MATLAB R2016a simulation software. 20 training samples from different ten people are selected, that is to say that two fingerprint images belonging to same finger for each person are adopted, but they are slightly different in appearance. These 20 images are numbered between 1 to 20. 10 fingerprint images in corresponding to the training samples are selected as test samples, which are numbered between 1 to 10. The test sample 1 corresponds to the training sample 1 and 2, that is to say that the serial numbers of the test sample and training samples are belonging to the same fingerprints with different forms. And so on, the test sample 10 corresponds to the training sample 9 and 10. The correspondence between training and test samples is shown in Fig. 14 and simulation results are shown in Fig. 15 and Fig. 16.

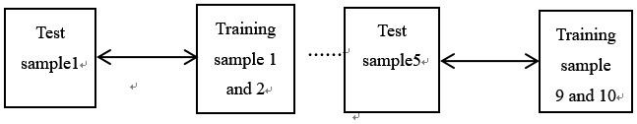

Fig. 14 Correspondence between training and test samples.

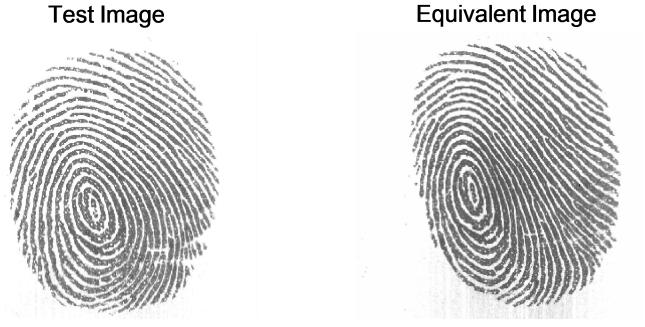

Fig. 15 Recognition results.

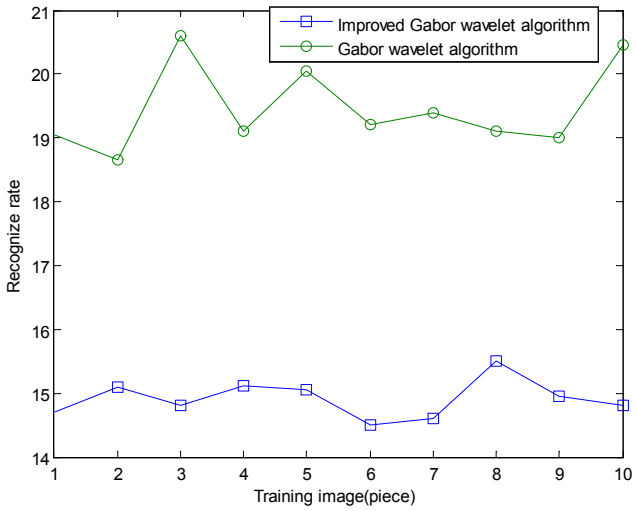

Fig. 16 Comparison of recognition time.

VII. Conclusions

Fingerprint identification is an important biometric identification and has wide application. In the whole process of identification, the enhancement of fingerprint is also crucial. Because the collected fingerprint images have noisy or other interference factors, an improved Gabor filter is adopted to realize the acquisition of fingerprint image enhancement. The improved filter can match the standard deviation and the filter size according to the different blocks, that is actually to use a lot of different filter to filter the images. In the process of feature extraction, the Gabor wavelet filter with five frequencies and eight channels are adopted to realize the feature extraction of enhanced fingerprint images without using the traditional detail points as characteristics. The final recognition phase utilizes the correlation of the feature space, and the experimental results prove the effectiveness of the proposed strategy.

References

[1] X. Liu, and Y. J. Jiang, "Fingerprint spoof detection using gradient co-occurrence matrix," *Engineering Letters*, vol. 25, no.4, pp. 360-365, 2017.

[2] R. Cappelli, M. Ferrara, and D. Maltoni, "Large-scale fingerprint identification on GPU," *Information Sciences*, no.306, pp. 1-20, 2015.

[3] P. W. Kwan, M. C. Welch, and J. J. Foley, "A knowledge-based decision support system for adaptive fingerprint identification that uses relevance feedback," *Knowledge-Based Systems*, no.73, pp. 236-253, 2015.

[4] J. Sang, H. Wang, Q. Qian, H. Wu, and Y. Chen, "An efficient fingerprint identification algorithm based on minutiae and invariant moment," *Personal & Ubiquitous Computing*, vol. 22, no.10, pp. 1-10, 2017.

[5] X. Liu, F. Zaki, Y. Wang, Q. Huang, and X. Mei, "Secure fingerprint identification based on structural and microangiographic optical coherence tomography," *Applied Optics*, vol. 56, no.8, pp. 2255, 2017.

[6] S. Ding, W. Bian, T. Sun, and Y. Xue, "Fingerprint enhancement rooted in the spectra diffusion by the aid of the 2D adaptive Chebyshev band-pass filter with orientation-selective," *Information Sciences*, vol. 415-416, pp. 233-246, 2017.

[7] G. J. Hou, G. D. Wang, Z. K. Pan, B. X. Huang, H. Yang, and T. Yu, "Image enhancement and restoration: state of the art of variational retinex models," *IAENG International Journal of Computer Science*, vol. 44, no.4, pp. 445-455, 2017.

[8] M. Galar, J. Derrac, D. Peralta, I. Triguero, and D. Paternain, "A survey of fingerprint classification Part I: Taxonomies on feature extraction methods and learning models, *Knowledge-Based Systems*, vol. 81, no.C, pp. 76-97, 2015.

[9] H. Al-Sahaf, M. Zhang, A. Al-Sahaf, and M. Johnston, "Keypoints detection and feature extraction: a dynamic genetic programming approach for evolving rotation-invariant texture image descriptors," *IEEE Transactions on Evolutionary Computation*, vol. 21, no.6, pp. 825-844, 2017.

[10] Z. Haddad, A. Beghdadi, A. Serir, and A. Mokraoui, "Wave atoms based compression method for fingerprint images," *Pattern Recognition*, vol. 46, no.9, pp. 2450-246, 2013.

[11] W. Lee, S. Cho, H. Choi, and J. Kim, "Partial fingerprint matching using minutiae and ridge shape features for small fingerprint scanners," *Expert Systems with Applications*, vol. 87, pp. 183-198, 2017.

[12] X. Fu, and J. Feng, "Minutia tensor matrix: a new strategy for fingerprint matching," *Plos One*, vol. 10, no.3, pp. e0118910, 2015.

[13] D. Bennet, and S. A. Perumal, "Fingerprint: DWT, SVD based enhancement and significant contrast for ridges and valleys using fuzzy measures," *Computer Science*, 2011.

[14] N. Onizawa, D. Katagiri, K. Matsumiya, W. J. Gross, and T. Hanyu, "Gabor filter based on stochastic computation," *IEEE Signal Processing Letters*, vol. 22, no.9, pp. 1224-1228, 2015.

[15] H. Zhao, and P. Xiao, "Optimal Gabor filter-based edge detection of high spatial resolution remotely sensed images," *Journal of Applied Remote Sensing*, vol. 11, no.1, pp. 015019, 2017.

[16] H. Ina, M. Takeda, and S. Kobayashi, "Fourier-transform method of fringe-pattern analysis for computer-based topography and interferometry, " *Review of Scientific Instruments*, vol. 72, no.12, pp. 156-160, 2015.

[17] T. Shen, Y. Tu, M. Li, and H. Zhang, "A new phase difference measurement algorithm for extreme frequency signals based on discrete time Fourier transform with negative frequency contribution," *Review of Scientific Instruments,* vol. 86, no.1, pp. 015104, 2015.

[18] K. G. Lore, A. Akintayo, and S. Sarkar, "LLNet: A deep autoencoder approach to natural low-light image enhancement," *Pattern Recognition*, vol. 61, pp. 650-662, 2017.

[19] Z. Z. Wang, and J. H. Yong, "Texture analysis and classification with linear regression model based on wavelet transform," *IEEE Transactions on Image Processing A Publication of the IEEE Signal Processing Society*, vol. 17, no.8, pp. 1421-1430, 2008.

[20] S. Hemalatha, amd S. M. Anouncia, "A computational model for texture analysis in images with fractional differential filter for texture detection," *International Journal of Ambient Computing & Intelligence*, vol. 7, no.2, pp. 93-113, 2016.

[21] S. Xia, and R. Wang, "A fast edge extraction method for mobile lidar point clouds," *IEEE Geoscience & Remote Sensing Letters*, vol. 14, no.8, pp. 1-5, 2017.

[22] Holmström, Lasse, L. Pasanen, R. Furrer, and S. R. Sain, "Scale space multiresolution analysis of random signals," *Computational Statistics & Data Analysis*, vol. 55, no.10 pp. 2840-2855, 2017.

[23] A. M. Al-Ssulami, "Hybrid string matching algorithm with a pivot," *Journal of Information Science*, vol. 41, no.1, pp. 82-88, 2015.

[24] A. Tanver, B. Carl, B. Widmer, G. Jia, C. S. Iliopoulos, L. Chang, and P. Solon, "Fast circular dictionary-matching algorithm," *Mathematical Structures in Computer Science*, vol. 27, no.2, pp. 143-156, 2015.

Bo-wen Zheng is currently a master student in School of Electronic and Information Engineering, University of Science and Technology Liaoning, China. His main research interest is image processing and pattern recognition.

Jie-sheng Wang received his B. Sc. And M. Sc. degrees in control science from University of Science and Technology Liaoning, China in 1999 and 2002, respectively, and his Ph. D. degree in control science from Dalian University of Technology, China in 2006. He is currently a professor and Master's Supervisor in School of Electronic and Information Engineering, University of Science and Technology Liaoning. His main research interest is modeling of complex industry process, intelligent control and Computer integrated manufacturing.

Yan-lang Ruan is currently a master student in School of Electronic and Information Engineering, University of Science and Technology Liaoning, China. His main research interest is image processing and pattern recognition.

Shu-Zhi Gao received the B. Sc. degree from Shenyang University of Chemical Technology, China in 1989, and received the M. Sc. degrees from Northeastern University, China in 2012. She is currently a professor and Ph. D. supervisor in Shenyang University of Chemical Technology. Her research interests include feedback control system, modeling of complex industry process and intelligent control.